*Al-Azhar Bulletin of Science Vol. 31, No. 1, (June) 2020, pp. 33-49*

# PREPARATION OF ACTIVATED CARBON FROM ION EXCHANGE RESIN WASTE AND ITS APPLICATION FOR MANGANESE REMOVAL FROM GROUNDWATER

**A.A.Swelam[1],Y.R.Gedamy[2] and A.A Elshahed[3]**

*Chemistry Department, Faculty of Science, Al-Azhar University, Cairo, Egypt.*
*2Hydrogeochemistry Dept., Desert Research Center, El-Matareya, Cairo, Egypt.*
Author to whome Correspondence should be addressed:
E-Mail: yahiagedamy2014@yahoo.com ahmedelshahed2018@gmail.com

## ABSTRACT

The present study aims to synthesize an activated carbon adsorbent (S-AC, P-AC and OH-AC) from polystyrene divinyl benzene waste under different carbonization temperature (450$^{o}$C and 900 $^{o}$C and activation conditions ($H_2SO4$, $H_3PO_4$ or NaOH). It being characterized and applied as an adsorbent for manganese removal from groundwater. FTIR results indicate that the changes in the peak intensities clear that the binding process was occurring on the surface of the adsorbent. Different factors such as solution pH, adsorbent dosage, contact time, temperature and Mn(II) initial concentration were investigated. The results showed that manganese adsorption capacity decreases with the increase of the carbonization temperature (900$^{o}$C) and of activating agent $H_2SO4$ > $H_3PO4$ >NaOH. Kinetically, it was shown that the activation temperature of 450$^{o}$C is the best temperature for activating the adsorbent carbons. The pseudo-first-order model is appropriate for predicting the adsorption process of Mn(II) onto the P-AC 450$^{o}$C, P-AC 900$^{o}$C and OH-AC 900$^{o}$C, while the pseudo-second-order model is appropriate for predicting the adsorption process of Mn(II) onto the both S-AC 450$^{o}$C, S-AC 900$^{o}$C, OH-AC 450$^{o}$Cand OH-AC 900$^{o}$C. Thermodynamic calculations affirmed that Mn(II) adsorption onto S-AC and P-AC was an endothermic process while onto OH-AC was exothermic process. Finally, the results suggested that the prepared S-AC has high adsorption capacities for Mn(II) compared with other adsorbents, such as P-AC and OH-AC. Therefore, S-AC 450$^{o}$Ccan be used in the groundwater treatment unit.

**Keywords:** Activated carbon; ion exchange resin; ground water.

## INTRODUCTION

Manganese (Mn) is abundant in the earth and exists as a component of more than 30 kinds of manganese oxides/hydroxide minerals. The presence of soluble manganese divalent ion Mn(II) is a salient feature in the groundwater [1].Manganese occurs naturally in surface water and groundwater, especially in oxygen depleted or anaerobic systems. The concentrations of manganese in groundwater are dependent upon a number of factors such as rainfall chemistry, aquifer lithology, geochemical environment and groundwater flow paths. Some of these factors can be highly variable over relatively small spatial and temporal scales. Manganese can be leached from overlying soils and minerals in underlying rocks as well as from the minerals of the aquifer itself. Mn(II) contaminated groundwater not only causes aesthetic and operational problems, such as water discoloration, laundry stains and pipes clogging, but also causes chronic poisoning to the human body and threats to the health [2]. The maximum contaminant level for manganese in drinking water has been established as 0.4 mg/L (WHO, 2011), [3].Therefore, effective removal of Mn(II) from the groundwater is necessary to provide safe drinking water.

In the developing countries, many water resources are polluted due to a diminished public awareness regarding environmental health, which leads to the indiscriminate disposal of waste or the discharge of effluent from industrial activity [4]. As the world population increases, there is an annual decline in the accessibility of clean and safe water, despite it being one of the most basic human necessities. More than half of a body's weight is composed of water, and it is important for cell growth, use as a body coolant, the protection of tissue from shock and damage, aiding in the digestion and absorption of food,

the removal of waste and the maintenance of a healthy weight [5].

Polystyrene divinyle benzene was produced from petroleum derivatives, it can use for some plastic industries as yogurt cans and the waste of polystyrene divinyle benzene is generated in large amount which leads to an environmental problem.

The principal goal of water treatment is to minimize the risks from biological, chemical and physical by reducing them to acceptable levels. This includes ensuring that the water is of high aesthetic quality; that is, the taste, odor, clearness, and color of the water do not cause offense to consumers. This also means guaranteeing that the water's chemical constituents do not cause operational problems in circulation systems [6]**.** Various techniques have been employed for the mitigation of Mn(II) including those of coagulation/flocculation [7], ion exchange [8], oxidation/filtration [9], adsorption [10] and membrane filtration [11].Due to the advantages of low cost and environmental friendliness, adsorption has been preferred worldwide.

The present work aims to introduce an inexpensive and renewable adsorbent for $Mn^{2+}$removal by converting exhausted resin with no commercial value into a promising adsorbent with the aid of mineral acids ($H_2SO_4$) (S-AC) and $H_3PO_4$(P-AC) and base NaOH (OH-AC) activation. The use of exhausted resin as renewable precursor for producing carbonaceous adsorbent materials in adsorption of $Mn^{2+}$ from aqueous solutions and groundwater in the batch-model process will diminish the large amount of exhausted resin, reduce environmental complications and produce value-added products. The adsorption parameters, kinetic and thermodynamic studies were performed to explore and predict the adsorption of $Mn^{2+}$ions onto the activated carbon.

## EXPERIMENTAL

### Reagents

Sulfuric acid ($H_2SO_4$), Phosphoric acid ($H_3PO_4$), sodium hydroxide (NaOH), hydrochloric (HCl), and manganese chloride ($MnCl_2$) were purchased from Sigma-Aldrich (St. Louis, MO, USA)**.** Waste polystyrene ascation exchange resin (Amberjet 1500) was supplied by Beihua Chemical Building Materials Co., Ltd. (Hebei, China).

### Preparation of the carbon composites

Polystyrene divinyl benzene obtained by polymerization of (styrene and divinyle benzene), the styrene ($C_8H_8$) is polymerized with itself and with divinyle benzene ($C_{10}H_{10}$)**,**prior to its use, the resin waste was successively rinsed with ethanol, 5% HCl solution, 5% NaOH solution, distilled water until the solution had a neutral pH to remove impurities, dried 60°C for 24h. Carbonization and activation were conducted in a horizontal cylindrical furnace (450°C or 900°C) for 3hrs(Qianqian et al., 2014) [12], after cooling the obtained carbon was mixed with concentrated sulfuric acid, phosphoric acid and powdered sodium hydroxide separately at a mass ratio of 1:3. Subsequently, after cooling the obtained carbons (S-AC, P-AC and OH-AC) was crushed and washed with distilled water until the solution had neutral pH, dried under vacuum.

### Batch adsorption experiments

Batch adsorption experiments were performed by shaking a mixture of a fixed amount of S-AC, P-AC and OH-AC separately with 25ml of manganese solution of a known concentration in a series of 100ml plastic bottles in a constant temperature shaker(Stuart CB302) for a known period of time. The suspensions were taken out at predetermined time intervals and centrifuged and analyzed using atomic absorption spectroscopy (SHIMADZUAA700). Several experiments were carried out with a variety of initial manganese concentrations, pH, contact time, adsorbent dosage, and temperature respectively. The amount of adsorbate that adsorbed onto the carbon at time t, $q_t$ (mg/g) and removal % from aqueous solution or groundwater are calculated from Eqs.1 and 2,respectively.

$$q_e = \frac{(C_0 - C_e)V}{W \times 1000} \quad \text{----------1}$$

The removal percentage yield (R%) =

$$\frac{C_0 - C_e}{C_0} \times 100 \quad \text{---------- 2}$$

Where, $C_o$ is the initial $Mn^{2+}$ ion concentration (mg/L) at equilibrium, Ce is the concentration of $Mn^{2+}$ at any time t, V is the volume of the manganese solution and w is the weight of carbon in (g). All experimental measurements were within ± 0.1% accuracy.

## RESULTS AND DISCUSSION

### Characterization of the synthesized carbons

To check about the structure of the new activated carbon before and after synthesized, a characterization must be done as the determination of the functional groups by FTIR. To better understand the differences among modified activated carbon produced by different modifiers, FTIR analysis was performed to identify surface functional groups on the carbon surfaces. Fig.(1) shows the FTIR of the activated carbon at $450^0$C (AC). The spectrum show a relatively strong band at 1573.91$cm^{-1}$ due to combined stretching vibrations of conjugated C=O group and aromatic rings [13]. The thermal activated carbon obtained at 450°C shows a small peak at 1697.36 $cm^{-1}$ characteristic of the C=O stretching vibration. The small intensity of this peak suggests a relatively low content of carboxylic groups as compared to other oxygen groups of carbon [14].Weak absorption band in all spectra at about 3047.53$cm^{-1}$ is ascribed to aromatic C-H stretching vibrations.

The FTIR spectrum of the S-AC (Fig.2) shows a band at 3433.29$cm^{-1}$ assigned to $OH^-$ stretching vibration. This finding is apparently due to the fact that $H_2SO_4$ initiated bond cleavage, leading to dehydration and elimination reactions that release volatile products such as water, acid, alcohol and other chemical substances. This is followed by partially aromatic city and re-combination of species to form a stronger cross-linked solid. In other words, $H_2SO_4$ breaks many bonds in aliphatic and aromatic species existed in the precursor material leading to liberation and elimination of many light and volatile substances causing partial aromatization and thus carbonization. In addition, if the spectrum of the modified activated carbon- $H_2SO_4$ is compared with activated carbon by means of sulfur related absorption bands, it is seen that 1165$cm^{-1}$ and new absorption bands appeared in the spectrum of S-AC sample at around 1072.42–1010.7$cm^{-1}$ assigned to asymmetric and symmetric stretching vibration of $SO_2$, respectively confirming the presence of surface $SO_2$ complexes [15 and 16]. However, the bands at 1010.7$cm^{-1}$ (C-O stretching in phenols, alcohols) and $H_2SO_4$ acid (-$SO_3$ groups).

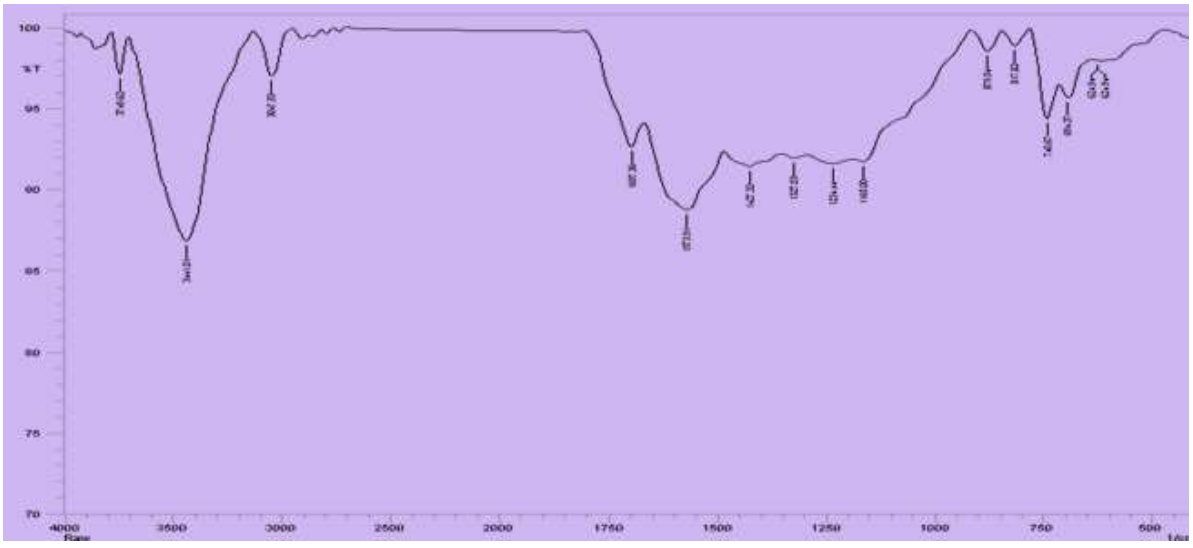


**Fig.1. FTIR spectrum of activated carbon at 450°C**

The band (Fig.3) at 1118.71cm$^{-1}$ could be assigned to stretching vibrations of C–O–C in aromatic esters. However, the peak at 1165cm$^{-1}$ can be assigned to the stretching vibration of hydrogen-bonded P=O groups from phosphates or polyphosphates, to the O–C stretches vibration in the P–O–C $_{(aromatic)}$ linkage. Therefore, oxygen and phosphorus enriched carbon were observed [17]. The observation of those extra peaks suggests that the biochar surface was well modified in situ with the pyrolysis process, and the properties of the as-obtained carbon surface was significantly enhanced by covering functional groups and mineral precipitants, and then greatly strengthen the adsorption performance [18].

As shown in Fig.4, many peaks were detected such as the broad peak at 3433.29cm$^{-1}$, low peak at 2916.37cm$^{-1}$, another peak at 1612.49cm$^{-1}$ with shoulder peak at 1705.07cm$^{-1}$ and a sharp peak at 1041cm$^{-1}$. These peaks correspond to the functional groups of O-H stretching, C-H, C=O and C-O stretching, respectively. These findings revealed that the OH-AC has OH, CO and COOH as their functional groups. The addition of NaOH onto AC may increase the amount of the functional groups on OH-AC, and NaOH has OH groups. The presence of these functional groups will make the surface of the adsorbents to be more hydrophilic and thus could enhance the adsorption of positive metal ions [19 and 20].

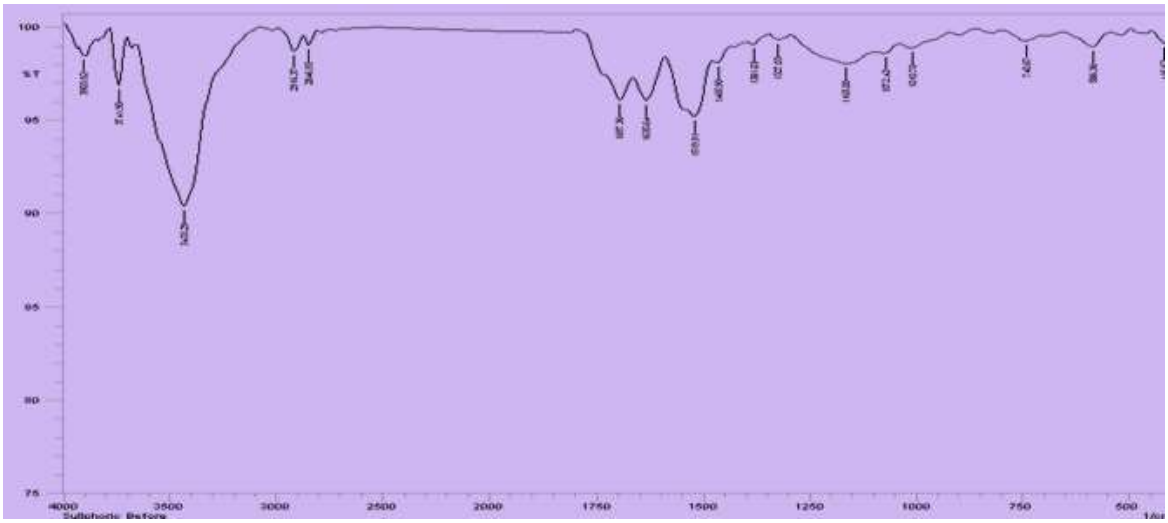

**Fig. 2. FTIR spectrum of sulphonic activated carbon (S-AC)**

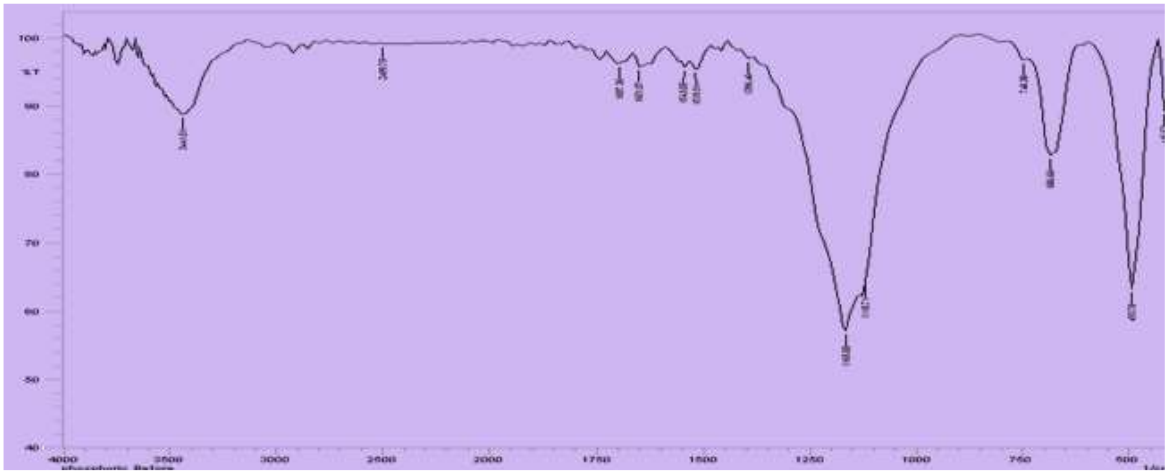

**Fig. 3.FTIR spectrum of phosphoric activated Carbone (P-AC)**

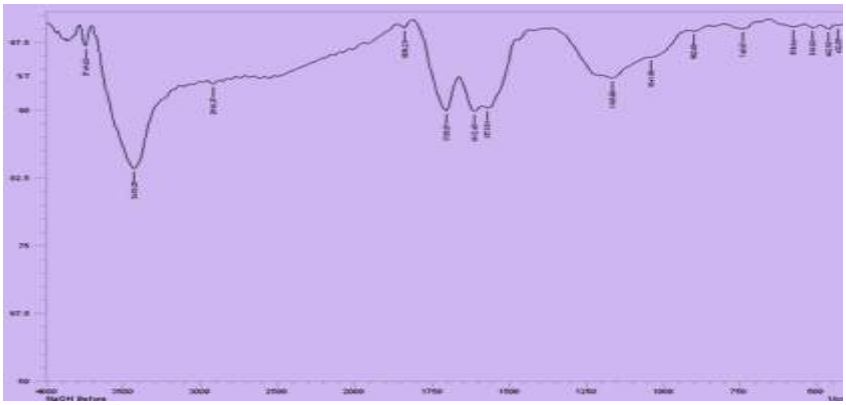

**Fig. 4.FTIR spectrum of Hydroxyl activated Carbone (OH-AC)**

Influencing factors on the removal efficiency of Mn(II)

**Effects of pH**

The effect of pH on the removal efficiency of Mn(II) was investigated in the range of 2 to 5.8. As shown in Fig.5, the removal efficiency and uptake of Mn(II) change by changing the pH value in the range of 2 to 5.8. However, in case of using S-AC, by increasing the pH value from 2 to 4, Mn(II) removal efficiency increases from 75 to 78% (18.5 to 19.5mg/g) and then decreases to reach 76% at pH 5.8.Where by using OH-AC, it was found that the Mn(II) removal efficiency decreases gradually from 72% (18mg/g) until reach to 67% (16.75mg/g) with increasing the pH from 2 to 5.8.Finally, at using P-AC, it was shown that, the Mn(II) removal efficiency increases as the pH increase until reach to 32%(8mg /g) at pH 3 and then decreases to 26 % (7mg/g) at pH 5.8. The low uptake of Mn(II) is observed at lower pH value and this can be attributed to the large quantities of protons that competes with Mn(II) ions at the adsorption sites. In other words, by increasing pH value, more positively charged Mn(II) ions are adsorbed by free binding sites due to a larger portion of dissociation of protons from functional groups, resulting in the promotion of adsorption capacity [21]. The maximum Mn(II) removal efficiency of 78% (pH= 4), 32% (pH= 3) and 72% (pH= 2) by the S-AC, P-AC and OH-AC, respectively. Then the worked resins are arranged in the order S-AC>P-AC>OH-AC with varying pH value.

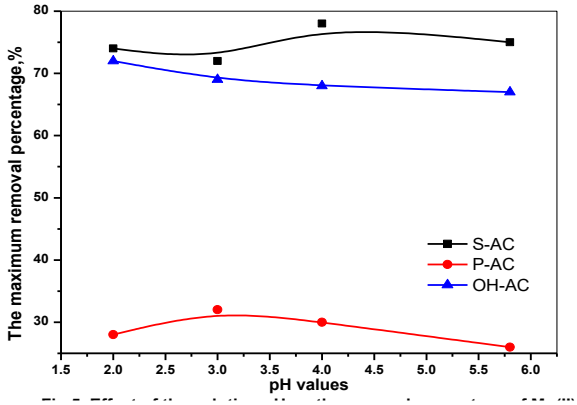


**Fog. 5 Effect of the solution pH on the removal percentage of Mn (II)**

**Effect of the adsorbent dosage**

Adsorbent dosage is a key parameter in the determination of removal efficiency and adsorption capacity. As the adsorbent dosage is increased, the available adsorption sites are also increasing; consequently, a better adsorption takes place. The effect of S-AC,P-AC and OH-AC dosage on the removal efficiency and uptake of Mn(II) from the solution can be studied in varying dosage 0.1, 0.2, 0.3 and 0.4 g at pH values 4,3 and 2 for S-AC,P-AC and OH-AC respectively, contact time 4hrs and at a constant concentration (50ppm) of the initial manganese solution (Fig.6).It was shown from Fig.6thatthere is an increase in the removal efficiency from 64 to 94%, 58to 88% and 18 to 60% for S-AC,OH-AC and P-AC respectively, with increasing the dosage from 0.1 to 0.4g.This can be attributed to the fact that by increasing the adsorbent dosage, the density of the available reactive groups on the adsorbent

surface for metal binding increases. While an opposite trend was observed where, the adsorption capacity decreases with increasing the adsorbent dosage. As the S-AC adsorbent dosage increases from 0.1 to 0.4 g, a decrease in the Mn(II) adsorption capacity from 8 to 2.94, 2.25 to 1.875 and 2.75 to 2.75 mg/g was observed, respectively. Thismay be due to the interference existed between the binding sites and adsorbent, or the insufficiency of Mn(II) ions in the solution with respect to available binding sites [21].

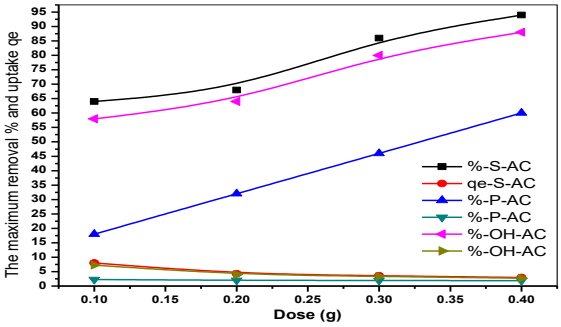


**Fig. 6. Effect of the carbon doses on the removal % and uptake of Mn(II)**

The effect of the initial solution concentration on the Mn(II) removal efficiency by the concerned adsorbent was studied at initial Mn(II) concentration varies between 50,75,100,125 and 150mg/L (Fig.7). The removal efficiency of Mn(II) onto S-AC450ºC, P-AC450ºC and OH-AC450ºC decreases from 64 to 58%, 18 to 12% and 58 to 54.6%, respectively, by increasing its initial concentration from 50 to 150mg/L. The removal efficiency is low at the highest concentration of Mn(II) due to the lower available adsorption sites in comparison with the number of Mn(II) ions. In brief, the performance of the S-AC, P-AC and OH-AC was evaluated by their removal percentages which were obtained as 64, 18 and 58% for S-AC, P-AC and OH-AC respectively, where the adsorption capacities of S-AC,P-AC and OH-AC change from 8 to 21.75 mg/g, 2.25 to 4.5mg/g and 7.25 to 20.5mg/g, respectively, by increasing Mn(II) initial concentration from 50 to 150 mg/L. This is confirmed with Saharan et al.,2019**[**22**]**who stated that the higher initial concentration of Mn(II) provides a driving force to overcome the mass transfer resistance between the aqueous and solid phases.

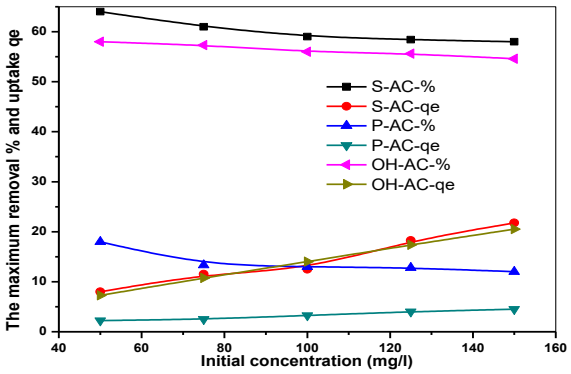


**Fig. 7. Effect of the initial concentration on the removal % and uptake of Mn(II)**

## Effect of contact time and activation temperature on the Mn(II) removal

The effect of contact time on the removal of Mn(II) from the groundwater was achieved at different time varies from 1 to 300min by two groups of activated carbons that have burned at two temperatures. The first group includes S-AC450°C, P-AC 450°C and OH-AC 450°C, and the second group includes S-AC 900°C, P-AC 900°C and OH-AC 900°C (Fig.8). It was observed that the removal of Mn(II) by S-AC 450°C,P-AC 450°C and OH-AC 450°C increases by increasing contact time till reaches to 0.975,0.95 and 0.725mg/g, respectively, at contact time 300min, while the removal of Mn(II) by S-AC 900°C,P-AC900°C and OH-AC 900°Cincreases by increasing contact time till reaches to 0.625, 0.425 and 0.725mg/g, respectively, at contact time 240min.The increase of the adsorption process at the beginning of the contact time may be due to a large number of active sites being available on the adsorbent surface for Mn(II) adsorption [23].

Fig.8. shows the effect of activation temperature (450 and 900°C) on the adsorption capacity of Mn(II) removal from the groundwater at fixed modification ($H_2SO_4$, $H_3PO_4$ and NaOH) and activation time of 300 and 240min, respectively. It was observed that, large manganese uptake capacity was obtained at the activation temperature up to 450°C and this may be due to the formation of a large amount of micro and mesopores. In other words, this may be also due to increase in surface area and total pore volume. In brief, further increase in activation temperature up to 900°C lead to a decrease in manganese uptake

capacity and this probably due to burning of micro and mesopores and matrix of carbon collapsed causing blockage of pores [24].

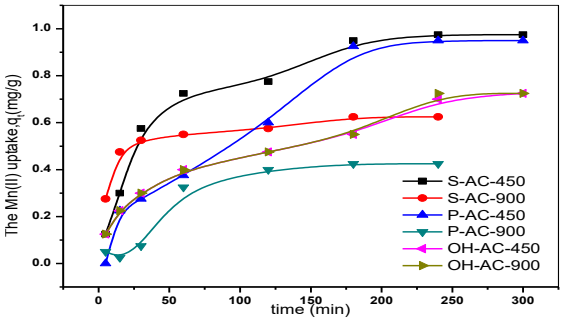


**Fig. 8. Effect of activation temperature and Contac time on the Mn(II) uptake (5m g/l, 296K., 25ml and 0.1 g carbon)**

**Adsorption kinetics studies**

Adsorption kinetics studies help in assessing the adsorption mechanisms in terms of order and rate constants, and provides useful information on possible rate control steps. Four kinetic models, pseudo-first-order [25], pseudo-second-order [26], Elovich[27] and intraparticle diffusion [28] were used to study the kinetics of the adsorption process of manganese by two groups of activated carbons, first group includes S-AC450ºC, P-AC 450ºC and OH-AC 450ºC, and second group includesS-AC900ºC, P-AC 900ºC and OH-AC 900ºC. The kinetic graphs obtained are depicted in figures Nos. 9,10, 11 and 12,respectively, and the linearized equation and plot parameters are summarized in table (1).

**The pseudo-first order model**

The pseudo-first order model equation is generally expressed as follows;

$$\frac{dq}{dt} = k_1(q_e - q_t) \quad \text{---------- 3}$$

Where $q_e$ and $q_t$ are the amount of metal sorbed per unit weight of sorbent at equilibrium and at any time t (mg/g), respectively, and $k_1$ is the rate constant of pseudo-first order sorption ($min^{-1}$). After integration and applying boundary conditions, for $t = 0$ and $q = 0$, the integrate form of Eq. (3) became

$$ln(q_e - q_t) = ln\, q_{e,1} - \frac{k_1 t}{2}.303 \quad \text{------ 4}$$

The values of rate constant $(k_1)$ and equilibrium capacity $(q_{(e,1,cal)})$ can be obtained from the slope and intercept of plotting log $(q_e - q_t)$ against time for three temperatures.

**The pseudo-second order model**

If the rate of sorption is a second order mechanism, the pseudo-second order chemisorption kinetic rate equation is expressed as;

$$\frac{dq}{dt} = k_2(q_e - q_t)^2 \quad \text{---------- 5}$$

Where $k_2$ is the rate constant of pseudo-second order sorption [g/(mg min)], $q_e$ is the amount of solute sorbet at equilibrium(mg/g) and $q_t$ is the amount of solute sorbet on the surface of the adsorbent at any time t (mg/g).

Integrating this equation (4) for the boundary conditions for $t = 0$, $q = 0$ gives

$$\frac{t}{q} = \frac{1}{k_2 q_{e,2}^2} + \frac{1}{q_{e,2}} t \quad \text{---------- 5, and}$$

$$h = k_2 q_{e,2}^2 \quad \text{---------- 6}$$

Where $h$ [mg/(g min)]means the initial adsorption rate, and the constants can be determined experimentally by plotting of $t/q$ against t.

**Elovich kinetic model**

The Elovich kinetic modelequation is generally expressed as follows;

$$q_t = \frac{1}{\beta} \ln(\alpha\beta) + \frac{1}{\beta} \ln t \quad \text{---------- 7}$$

Where α is the initial adsorption rate in mg/(g.min) and β (g/mg) is the desorption constant related to the extent of the surface coverage and activation energy for chemisorption. Both the kinetic constants α and β will be estimated from the slope and intercept of the plot of $q_t$ versus ln(t).

**Intra-particle diffusion equation**

The intra particle diffusion equation is the following;

$$q_t = K_{int}\, t^{0.5} + C \quad \text{---------- 8}$$

Where $K_{int}$ is the intraparticle diffusion rate coefficient (mg $g^{-1}$ $min^{½}$) and $C$ (mg $g^{-1}$) provides an idea about the thickness of the

boundary layer.The $K_{int}$ and $C$ can be obtained from the slope and intercept of a straight line plot of $q_t$ versus $t^{0.5}$.

It was shown that the data obtained from the adsorption experiments of Mn(II) onto the first group of activated carbons at 450ºC that namely; S-AC450ºC, P-AC450ºC and OH-AC450ºC were summarized in table (1). As in the table(1), it is evident that the correlation coefficient ($R^2$) values obtained by pseudo-first-order model are 0.89775 and 0.79645 for Mn(II) adsorption onto S-AC450ºC and OH-AC450ºC, respectively, which are low in comparison with that obtained by pseudo-second-order model (0.99015 and 0.95541) for S-AC450ºC and OH-AC450ºC, respectively.

The lower values of the obtained$R^2$ from the pseudo-first-order model indicate the unsuitability of this model for predicting the adsorption of Mn(II) onto the S-AC450ºC and OH-AC450ºC.Thus,pseudo-second-order model is appropriate for predicting the adsorption process of Mn(II) onto the S-AC450ºC and OH-AC450ºC.

On the other hand, the obtained correlation coefficient ($R^2$) value by pseudo-first-order model of Mn(II) adsorption onto the P-AC450ºC (0.96642)is higher than that obtained by the pseudo-second-order model (0.82767) showing a good fit for pseudo-first-order model for adsorption of Mnonto the P-AC450ºC.

The Elovich coefficients can be obtained from the linear plot of qt versus ln(t). If the adsorption of manganese ions by using S-AC450ºC, P-AC450ºC and OH-AC450ºC carbons fits the Elovich model, a plot of qt versus ln(t) should yield a linear relationship with a slope of (1/β) and an intercept of 1/βln(αβ) [29]. As in table1, the correlation coefficients obtained by Elovich model showed good linearity with both S-AC450ºC ($R^2$= 0.97284) and OH-AC450ºC ($R^2$=0.93627), which means that this model is a good model for adsorption of Mn(II) on S-AC 450ºC and OH-AC 450ºC.

On the other hand, it can also be observed that Elovich model gave an account of the occurrence of desorption process, while this model was poor fits for P-AC450ºC carbon ($R^2$=0.86538). It is clear that the correlation coefficients obtained were almost linear which indicated that Elovich model fitted well for adsorption by S-AC 450ºC and OH-AC 450ºC and not fitted for adsorption byP-AC 450ºC. The model gave a good correlation for adsorption on highly heterogeneous surface carbon. Besides, it is also shown that along with surface adsorption, chemisorption was also a dominant phenomenon taking place [30].

The obtained correlation coefficients ($R^2$) of the intra-particle diffusion are 0.86338, 0.93966 and 0.98133, suggesting that two or more steps are involved in Mn(II) adsorption onto the S-AC450ºC, P-AC450ºC and OH-AC450ºC, respectively. Higher values of the obtained$R^2$ from intra-particle diffusion model indicate that this model fitted well for adsorption of Mn(II) by P-AC 450ºCand OH-AC 450ºC, respectively, while the lower value indicates the unsuitability of this model for predicting the adsorption of Mn(II) onto the S-AC 450ºC adsorbent.

Noteworthy to mention that, the adsorption processes of Mn(II) onto the second group of carbons were evaluated with different kinetic models. A plot of ln(qe-qt) versus t (Fig.9) gave a linear curve, and the obtained results showed that the first-order rate constant ($k_1$) was found to be 0.01383, 0.02564 and 0.00658 for adsorption of manganese ions onto S-AC900ºC, P-AC 900ºC and OH-AC 900ºC, respectively, with a correlation coefficient values ($R^2$) of 0.67014,0.95482 and 0.95709 for S-AC900ºC, P-AC 900ºC and OH-AC 900ºC, respectively. The lower correlation coefficient value suggests that the pseudo-first-order model is not appropriate for Mn(II) adsorption onto S-AC 900ºC, while the high correlation coefficient values suggest that the pseudo-first-order model is best appropriate for Mn(II) adsorption onto both P-AC 900ºC and OH-AC 900ºC.

The pseudo second-order model describes the adsorption equilibrium capacity as well as the chemisorptive behavior of the adsorption process. A plot of $t/q_t$ versus t (Fig.10) gave a linear curve and high $R^2$ value of 0.93727and 0.92893 for S-AC 900ºC and OH-AC 900ºC, respectively. These results implied that the pseudo-second-order model was best described for Mn(II) adsorption onto S-AC 900ºC and

OH-AC 900ºC, while it is not fitting for the adsorption of Mn(II) onto P-AC 900ºC ($R^2$ = 0.00424).Also, this suggests that the rate-limiting step of the adsorption process is chemical adsorption.

The Elovich model helps in understanding the kinetics of chemisorptions of the adsorb ate on the solid surface of the adsorbent. The values for α and β are obtained from a plot of $q_t$ versus l nt (Fig.11), and their values are presented in table (1).As in table 1, the obtained correlation coefficients by Elovich model was 0.91396, 0.86312 and 0.78213 for OH-AC 900ºC, S-AC900ºC and P-AC900ºC, respectively, which means that the Elovich model was fitted for adsorption of Mn(II) onto OH-AC 900ºC, while it was poor fitted for adsorption of Mn(II) ontoS-AC900ºC and P-AC900ºC.

Weber and Morris's intra-particle diffusion model helps to identify the diffusion mechanism and the rate-limiting step. The boundary layer thickness(C) and intra-particle diffusion rate constant ($k_{int}$) can be deduced from the intercept and slope of the plot of $q_t$ versus the square root of time ($t^{1/2}$), respectively. It was observed from the plot that, the adsorption process takes place in two phases. The first phase depicts the rapid adsorption of manganese ions over a certain period of time, whereas the adsorption rate became slower in the second phase. This could be due to the chemisorptive interactions during the first stages of the adsorption process followed by intra-particle diffusion in the second stage. From Fig.12, the lines failed to pass through the origin, which suggests that intra-particle diffusion cannot be considered the rate-limiting step. As in table 1, the obtained correlation coefficients by intra-particle diffusion model was 0.96744, 0.85729 and 0.65638 for OH-AC 900ºC, P-AC 900ºC and S-AC 900ºC, respectively, which means that the intra-particle diffusion model was fitted for adsorption of Mn(II) onto OH-AC 900ºC, while it was poor fitted for adsorption of Mn(II) onto P-AC 900ºC and S-AC 900ºC.

The previous results were shown that the activation temperature (450°C) is the best temperature for activation of adsorbent carbons. The pseudo-first-order model is appropriate for predicting the adsorption process of Mn(II) onto the P-AC 450ºC,P-AC 900ºCandOH-AC 900ºC, while the pseudo-second-order model is appropriate for predicting the adsorption process of Mn(II) onto the both S-AC 450ºC, S-AC 900ºC, OH-AC 450ºCand OH-AC 900ºC.Also, Elovich modelis appropriate for predicting the adsorption process of Mn(II) onto the S-AC 450ºC, OH-AC 450ºC and OH-AC 900ºC. Finally, the intra-particle diffusion model is appropriate for predicting the adsorption process of Mn(II) onto the OH-AC 450ºC,P-AC 450ºC and OH-AC 900ºC.

**Table 1.Kinetic parameters of $Mn^{2+}$ adsorption in aqueous solutions using different carbons**

| Kinetic model | S-AC (450 Cº ) | S-AC (900 Cº ) | P- AC (450 Cº ) | P-AC (900 Cº ) | OH- AC (450 Cº ) | OH-AC (900Cº) |
|---|---|---|---|---|---|---|
| **PFO** | | | | | | |
| **qe,1,cal** | **0.8612** | **0.2160** | **0.9006** | **0.544** | **0.688** | **0.5478** |
| **$k_1$** | **0.0177** | **0.0138** | **0.0088** | **0.0256** | **0.0109** | **0.0065** |
| **$R^2$** | **0.8977** | **0.6701** | **0.9664** | **0.9548** | **0.7964** | **0.9570** |
| **PSO** | | | | | | |
| **qe,2,cal** | **1.118** | **0.7881** | **1.429** | **1.177** | **0.8007** | **0.7566** |
| **$k_2$** | **0.0238** | **0.0641** | **$5.5X10^{-3}$** | **0.0024** | **0.0246** | **0.0296** |
| **h** | **0.0298** | **0.0398** | **0.0112** | **0.0034** | **0.0158** | **0.0169** |
| **$R^2$** | **0.9901** | **0.9372** | **0.8276** | **0.0042** | **0.9554** | **0.9289** |
| **Elovich** | | | | | | |
| **β** | **4.436** | **11.550** | **3.555** | **7.917** | **6.888** | **7.160** |
| **α** | **0.0757** | **0.7746** | **0.0284** | **0.0185** | **0.0479** | **0.0497** |
| **$R^2$** | **0.9728** | **0.8631** | **0.8653** | **0.7821** | **0.9362** | **0.9139** |
| **Intraprticle diffusion** | | | | | | |
| **$K_{int}$** | **0.0540** | **0.0244** | **0.0625** | **0.0409** | **0.0385** | **0.0403** |
| **C** | **0.1581** | **0.3261** | **-0.0495** | **-0.0815** | **0.0691** | **0.0587** |
| **$R^2$** | **0.8633** | **0.6563** | **0.9396** | **0.8572** | **0.9813** | **0.9674** |

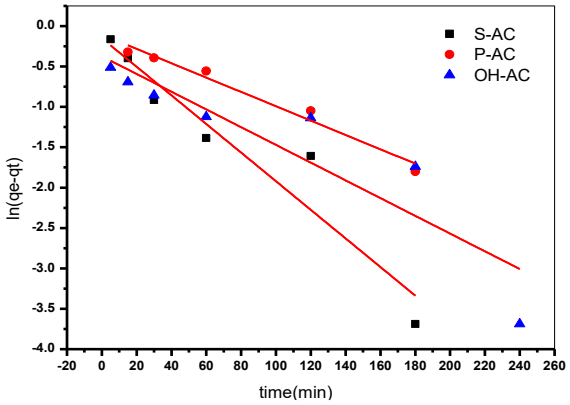


**Fig. 9. Pseudo-first order plots of Mn(II)**

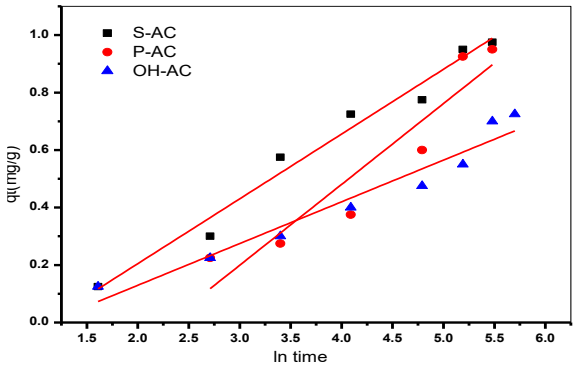


**Fig. 10. Pseudo-second order plots of Mn(II)**

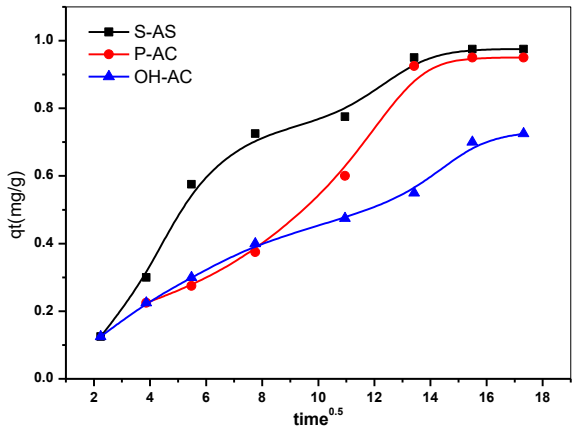


**Fig. 11. Elovich plots of Mn(II) 450°C.**

## Effect of temperature on the removal% of Mn(II)

The effect of temperature is accepted as a major factor affects the adsorption. The effect of the solution temperature on the removal% of Mn(II) by the activated carbons S-AC,P-AC and OH-AC can be studied at temperature varies from 296 to 320k (Fig.13).As shown inFig.13,the removal% of Mn(II) by both S-AC and P-AC increases with increasing temperature till reaches to the maximum removal% at the temperature 316k and then decreases with increasing temperature .The decrease in removal% might be due to the reduction of the attraction forces between the adsorbate and adsorbent as a result of increase in temperature [31]. In addition, the high temperature can also promote the adsorption process by accelerating molecular thermal motion to facilitate the contact between target ions and the sorbent [32]. On the other hand, it was shown that the removal% of the Mn(II) by OH-AC decreases with increasing temperature .

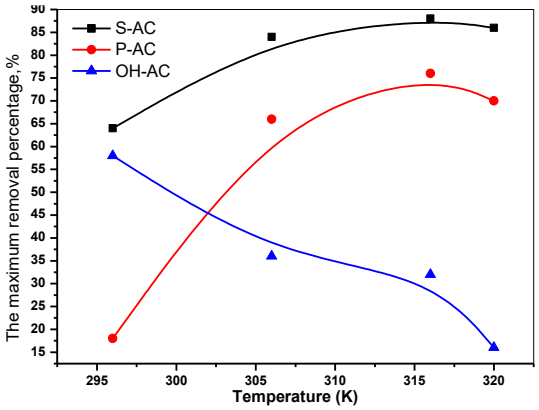


**Fig. 13. Effect of the solution temperature on the removal percentage of Mn(II)**

## Thermodynamic parameters

Data given from the thermodynamic studies are important for predicting the adsorption mechanism of heavy metals from the polluted water and thiscan be achieved at various temperatures (296, 306, 316 and 320 K).The thermodynamic parameters in particular are;Gibbs free energy ($\Delta G^o$), enthalpy change ($\Delta H^o$)and standard entropy change ($\Delta S^o$) are computed by Eqs. 9 and 10.

$$\Delta G^o = -RT\ln K_d \quad \text{----------} \quad (9)$$

$$\ln K_d = R - RT \quad \text{----------} \quad (10)$$

The thermodynamic results of manganese adsorption by S-AC, P-AC and OH-AC were shown in both Fig.14 and table 2.The obtained negative $\Delta G°$ values indicate favorable, spontaneous manganese adsorption by S-AC at the temperatures306, 316 and 320K, whereas,

the manganese adsorption by both P-AC and OH-AC at all the four temperatures 296, 306, 316 and 320K was non spontaneous. The obtained positive ΔS° values indicate an increase in the randomness of the solid/liquid interface, with structural changes in the adsorbate/adsorbent system [33]. In other words, the positive ΔH° values confirm the endothermic nature of the adsorption processes [34]using both S-AC and P-AC.

The Negative value of ΔHº affirmed the exothermic nature of the adsorption procedure by OH-AC. This is this agrees with Das et al., 2014, [35], who stated that, the enthalpy value in the interval ranging from 2 to 20 kJ $mol^{-1}$ points to physisorption, while the value inside 20–400 kJ $mol^{-1}$ characterizes chemisorption. Hence, the obtained enthalpy values show in table(2) confirm that the chemisorption characteristics governs the uptake process of Mn(II) by both S-ACand P-AC. On the other side, the negative entropy value shows that diminished disorder ensues at the solid/solution interface throughout the adsorption procedure [36] by OH-AC material.

**Table 2. Thermodynamic parameters of Mn(II) adsorbtion by S-AC, P-AC and OH-AC**

| Temp. | Temp.K | $\Delta G^0$ KJ/Mol | $\Delta H^0$ KJ/Mol | $\Delta S^0$ J/mol.K |
|---|---|---|---|---|
| | 296 | 1.966 | | |
| | 306 | -0.692 | | |
| | 316 | -0.159 | | |
| | 320 | -1.141 | | |
| | 296 | 7.144 | | |
| | 306 | 1.839 | | |
| | 316 | 0.615 | | |
| | 320 | 1.434 | | |
| | 296 | 2.636 | | |
| | 306 | 4.991 | | |
| | 316 | 5.622 | | |
| | 320 | 8.101 | | |

The obtained results suggest that S-AC has high adsorption capacities for $Mn^{2+}$ compared with other adsorbents, such as P-AC and OH-AC. Therefore, S-AC can be used in groundwater treatment unit to give satisfactory results such as obtaining high removal efficiency.

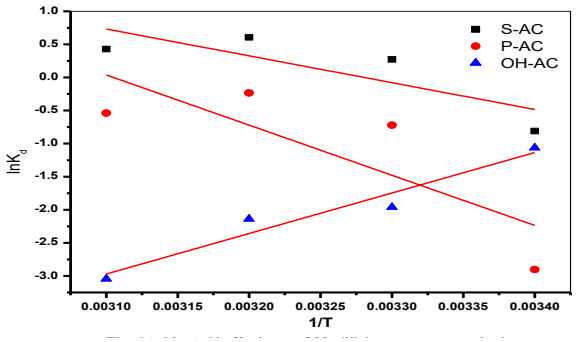


**Fig. 14. Van't Hoff plots of Mn(II) in aqueous solutions**

## Treatment of the polluted groundwater in the Northwest coast area-Egypt

In this study, some of polluted groundwater samples were collected from the Northwest coast areaFig.15, and transported to the Desert Research Center laboratories to analyze based on the international standard methods according to Rainwater and Thatcher, 1960[37] and Fishman and Friedman, 1985[38] to determine both the major and trace constituents, respectively, in the collected water samples (Table3).As shown in table 3, it was noticed that some groundwater samples are unsuitable for drinking purposes as they have $Mn^{+2}$concentration more than the safe limit (0.4mg/L; WHO,2011). So, it must be using an adsorbent (as S-AC) to decrease the concentration of manganese ion from this polluted groundwater to less than 0.4mg/L. To achieve this aim, the factors that affect on the adsorption process of $Mn^{+2}$ from groundwater have been studied as the following;

**Table 3 The concentrations of Mn(II) and Zn(II) in the collected groundwater samples in the study area**

| Sample No | Conc. of Zinc (mg/L) | Conc. of Mn (mg/L) |
|---|---|---|
| 1 | 0.122 | 0.126 |
| 2 | 1.870 | 0.876 |
| 3 | 0.919 | 0.028 |
| 4 | 0.675 | 0.154 |
| 5 | 0.150 | 0.024 |
| 6 | 0.256 | 0.190 |
| 7 | 0.016 | 0.008 |
| 8 | 0.457 | 0.130 |
| 9 | 0.363 | 0.015 |
| 10 | 0.011 | 0.014 |
| 11 | 1.820 | 0.013 |
| 12 | 0.289 | 0.017 |
| 13 | 0.264 | 0.015 |
| 14 | 0.363 | 0.461 |

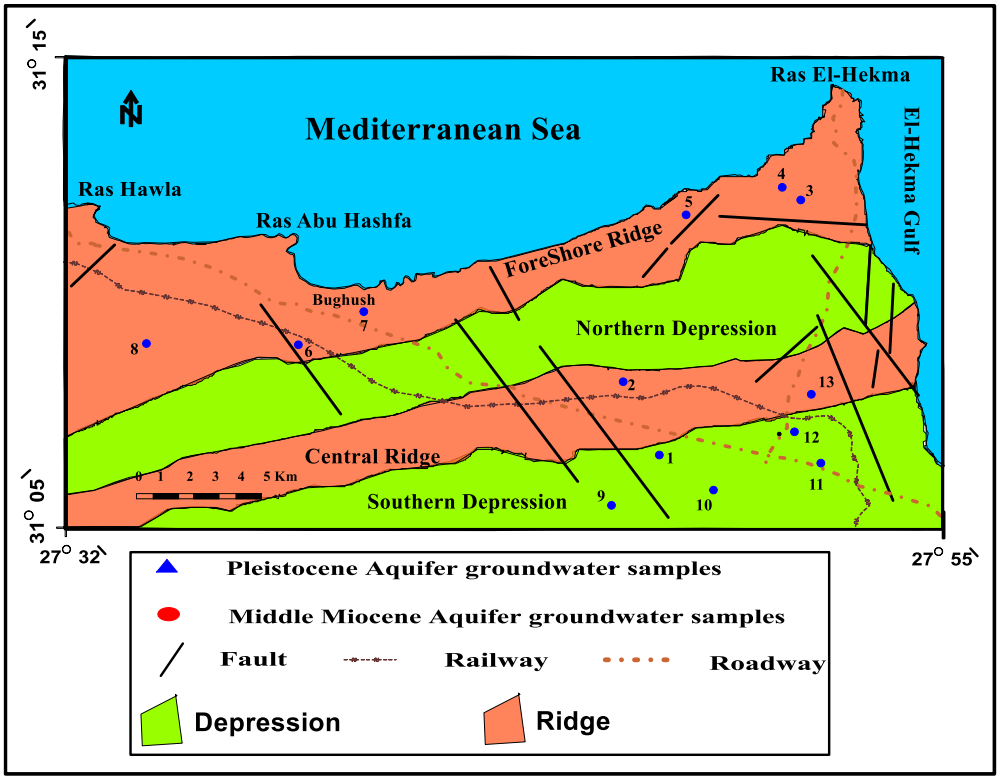


**Fig.15 Groundwater samples sites location map**

## Effect of the adsorbent dosageon the removal% of Mn(II)

Adsorbent dosage has significant impact on the adsorption process as it determines the sorbent-sorbated equilibrium of the system [39]. The effect of the adsorbent dosage on the removal% of Mn(II) from the polluted groundwater by S-AC was carried out at adsorbent dosages varies from 0.1 to 0.4mg for two groundwater samples Nos. (2 and 14) at pH 4.0and contact time 4h.Fig.16 shows that manganese ions removal efficiency from samples Nos.2 and 14 increased with increasing S-AC dosages from 0.1 to 0.4g.The removal efficiency of Mn(II) by S-AC increases gradually by increasing S-AC dosage till reach to the maximum values(~37% and 17.57%at samples Nos. 2 and 14, respectively. In brief, at constant initial Mn(II) concentration, with increasing the adsorbent dosage, the adsorption sites remain unsaturated. On the conrary, at low adsorbent dosage, all the active sites were exposed and occupied completely leading to saturation of the surface.

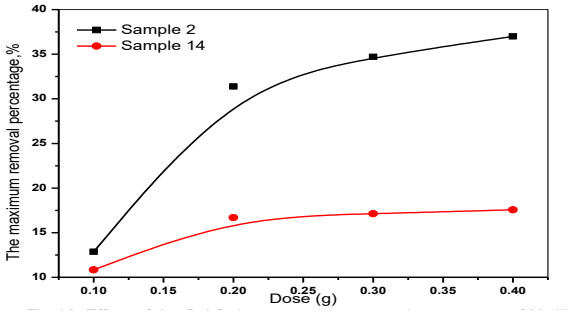


**Fig. 16. Effect of the S-AC dosage on the removal percentage of Mn(II) from groundwater samples 2 and 14**

## Effect of the initial manganese concentration on the removal% of Mn(II)

To evaluate the effect of the initial manganese concentration on the removal capacity of the concerned adsorbent, the experiments were carried out with varying initial manganese concentrations (0.876 and 0.431mg/L)at 296k,pH 4.0and 0.4g S-AC adsorbent dosage till 4h of contact time (Fig.17). It was observed that, a gradual increase in the adsorption capacity of S-AC from 0.0111 to 0.0297mg/g and from 0.0025 to 0.0037mg/g of samples Nos.2 and 14,

respectively, and then decreases at high concentration to reach to 0.019 and 0.0033mg/g, respectively, with increase of initial manganese concentration. An increase in adsorption by S-AC with increase in manganese concentrations might be due to relative increase in mass transfer[40].

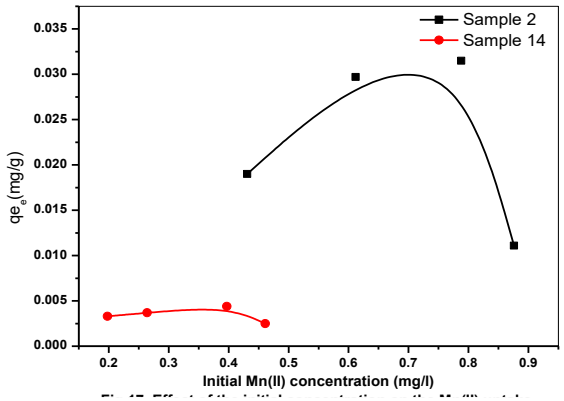


**Fig. 17. Effect of the initial concentration on the Mn(II) uptake from groundwater samples 2 and 14.**

increasing of swelling, the interaction between the adsorb ate ions and the binding sites on the adsorbent surface increases and this deal with increase the removal adsorption. In other words, the adsorption capacity increases at high temperature esdue to the superior diffusion rate of the metal ions and the lower solution viscosity of the adsorbent particles [41].

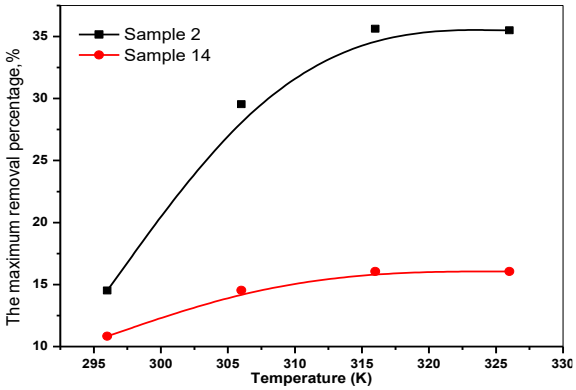


**Fig. 18. Effect of the solution temperature on the removal percentage of Mn(II) from different grouundwater samples 2 and 14**

### Effect of temperature on the removal% of Mn(II)

Temperature is one of the most important factors, which might have a critical role on the proceeding of the adsorption process of Mn(II) from polluted groundwater. The effect of the temperature on the $Mn^{2+}$adsorption process from polluted groundwater onto the S-AC was investigated at 296, 306, 316 and 320K,S-AC adsorbent dosage0.4g and initial Mn(II) concentrations0.876and 0.431mg/Lfor samples Nos.2&14 and pH 4.0atcontact time 4h (Fig.18).As shown inFig.18, the processes of Mn(II) removal% from groundwater sample No.2 increases from 14.51 to 35.62% by increasing temperature from 296 to 316K and then slightly decreases till reaches to 35.5% at temperature 320k.While for groundwater sample No.14, the processes of Mn(II) removal% increases from 10.84 to 16.05% with increasing temperature from 296 to 316kand the removal% still constant(No change was observed) with increasing temperature till reach to 320k.This increase of the removal adsorption with increasing temperature may be due to the development of new pores in the adsorbent and reduction in the viscosity of the medium. With

### Thermodynamic parameters for $Mn^{2+}$ adsorption onto the S-AC carbon from different groundwater samples.

The estimated thermodynamic parameters values of the Van't Hoff equation (Eq.9) for $Mn^{2+}$ adsorption on the S-AC from groundwater samples Nos.2 and 14, were listed in the table (4) and represented in Fig.19.The positive values of ΔG° (Eq.10) at all four temperatures indicate that the adsorption reaction requires energy to carry out and also, the adsorption process has a non-spontaneous nature. The decrease of ΔG° change values as a function of temperature indicates that the adsorption may be favored at high temperature [42]. The positive ΔS° values indicate an increase in the randomness of the solid/liquid interface with structural changes in the adsorb ate/adsorbent system [43]. Also, the positive ΔH° values confirm that the endothermic nature of the adsorption processes were corroborate with the isotherm results. In brief, the adsorption capacities increase with the increase in temperature due to the increase in $Mn^{2+}$ mobility and diffusion through the porous structures of the S-AC carbon, overcoming the activation energy.

**Table 4. Thermodynamic parameters for Mn(II) adsorption onto the S-AC carbon from groundwater**.

| Sample No. | ΔH kJ/Mol | ΔS J/Mol.K | $R^2$ | ΔG kJ/Mol | | | |
|---|---|---|---|---|---|---|---|
| | | | | Temperature K | | | |
| | | | | 296K | 306K | 316K | 326K |
| 2 | 36.223 | 88.800 | 0.7846 | 10.416 | 8.266 | 7.123 | 7.134 |
| 14 | 11.973 | 4.468 | 0.7185 | 10.850 | 10.025 | 9.738 | 9.738 |

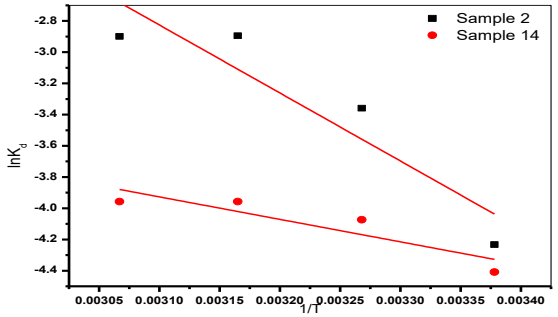


**Fig. 19. Van't Hoff plots of manganese adsorption in different groundwater samples (S-2 and S-14)**

## CONCLUSION

In the present study, polystyrene divinyl benzene (Amberjet 1500 cation exchange resin) waste-derived carbon at 450ºC and 900ºC was prepared, characterized and applied as a cost-effective adsorbent for manganese (Mn) removal from the polluted groundwater after the modification with $H_2SO_4$ (S-AC), $H_3PO_4$ (P-AC) and NaOH (OH-AC). The effects of the functional parameters such as solution pH, contact time, temperature and initial concentration on the Mn (II) removal efficiency by the activated carbons were evaluated. The activated carbons exhibited greater adsorption efficiency at 450ºC than at 900ºC, this may be due to its porosity and surface functionality. The maximum adsorption was achieved at pH values 4, 3 and 2, temperature 316, 316 and 296 K, carbon dosage 0.4g, initial manganese concentration 150mg/l and contact time of 4, 4 and 5 h with modified activated carbons S-AC, P-AC and OH-AC, respectively at 450ºC.While, with activated carbons at 900ºC, the optimum contact times was 3, 3 and 4h using S-AC, P-AC and OH-AC, respectively. Kinetically, it was shown that the temperature 450°C is the best temperature for activation of adsorbent carbons. It was observed that, the pseudo-first-order model is appropriate for the adsorption process of Mn(II) onto the P-AC 450ºC,P-AC 900ºCandOH-AC 900ºC, while the pseudo-second-order model is appropriate for the adsorption process of Mn(II) onto the both S-AC 450ºC, S-AC 900ºC, OH-AC 450ºCand OH-AC 900ºC.Also, Elovich modelis appropriate for the adsorption process of Mn(II) onto the S-AC 450ºC, OH-AC 450ºC and OH-AC 900ºC. Finally, intraparticle diffusion models are appropriate for the adsorption process of Mn(II) onto the OH-AC 450ºC,P-AC 450ºC and OH-AC 900ºC. Thermodynamics calculations affirmed that Mn(II) adsorption processes onto S-AC and P-AC was endothermic processes while the adsorption processes onto OH-AC was exothermic process. The negative ΔG° values indicate that the adsorption was favorable and spontaneous adsorption on S-AC at the three temperatures 306, 316 and 326K, whereas, the manganese adsorption by both P-AC and OH-AC at all four temperatures 296, 306, 316 and 326K was non spontaneous. In brief, the prepared S-AC, P-AC and OH-AC can be considered as an effective adsorbent for Mn(II) removal from aqueous solutions and polluted groundwater. While, the obtained results indicated that S-AC has high adsorption capacities for $Mn^{2+}$ compared with other adsorbents, such as P-AC and OH-AC. Therefore, S-AC 450ºCcan be used for groundwater treatment as it gives higher satisfactory removal efficiency.

## REFERENCES

[1] Y. Guo, T. Huang, G. Wen, X. Cao The simultaneous removal of ammonium and manganese from groundwater by iron-manganese co-oxide filter film: the role of chemical catalytic oxidation for ammonium removal, Chem. Eng. J., 308 (2017), pp. 322-329

[2] A.K. Rose, L. Fabbro, S. Kinnear Hydrogeochemistry in a relatively unmodified subtropical catchment: insights regarding the health and aesthetic risks of manganese, J. Hydrol.: Reg. Stud., 13 (2017), pp. 152-167

[3] World Health Organization (WHO, 2011). The guidelines for drinking waterquality, 4thed.

[4] A.R. Khalit; Current State of Water Environment in Malaysia (2016) http://www.wepa-

db.net/pdf/0712forum/paper09.pdf [July 27, 2016]

[5] J.R. De Palma, J.D. Pittard; Body Water-body Weight (2001) http://www.hemodialysis-inc.com/articles/bodywater.pdf (Accessed 09 April 2017)

[6] P. Payment, Goals of Water Treatment and Disinfection: Reduction in Morbidity and Mortality, Dlm. Willie O.K. Grabow (pnyt.). Water and Health (2009) 122–133 Encyclopedia of Life Support Systems (EOLSS), United Kingdom.

[7] X.M. Tang, H.L. Zheng, H.K. Teng, Y.J. Sun, J.S. Guo, W.Y. Xie, Q.Q. Yang, W. ChenChemical coagulation process for the removal of heavy metals from water: a review, Desalin. Water Treat., 57 (2016), pp. 1733-1748

[8] O. Kononova, G. Bryuzgina, O. Apchitaeva, Y. KononovIon exchange recovery of chromium (VI) and manganese (II) from aqueous solutions, Arab. J. Chem. (2015), pp. 1-8

[9]X. Du, K. Zhang, B. Xie, J. Zhao, X. Cheng, L. Kai, J. Nie, Z. Wang, G. Li, H. LiangPeroxymonosulfate-assisted electro-oxidation/coagulation coupled with ceramic membrane for manganese and phosphorus removal in surface water Chem. Eng. J., 365 (2019), pp. 334-343

[10] B. Al-Rashdi, C. Somerfield, N. HilalHeavy metals removal using adsorption and nanofiltration techniques, Sep. Purif. Rev., 40 (2011), pp. 209-259

[11] C.M. Chew, M.K. Aroua, M.A. Hussain, W.M.Z.W. IsmailPractical performance analysis of an industrial-scale ultrafiltration membrane water treatment plant, J. Taiwan Inst. Chem. Eng., 46 (2015), pp. 132-139

[12]Qianqian Shi, Aimin Li, Qing Zhou, ChendongShuang, Yan Ma; Utilization of *waste*cation exchange *resin* to prepare *carbon*/iron composites for the *adsorption* of contaminants in water, Journal of Industrial and Engineering Chemistry 20 (2014) 4256-4260.

[13]J. Coates; Interpretation of infrared spectra, a practical approach; R.A. Meyers (Ed.), Encyclopedia of analytical chemistry, John Wiley & Sons Ltd, Chichester (2000) 10815-10837.

[14] E. Apaydın-Varol, A.E. Pütün; Preparation and characterization of pyrolytic chars from different biomass samples, J. Anal. Appl. Pyrolysis, 98 (2012) 29-36,

[15]ÖzgülGerçel, Adnan Özcan, A. SafaÖzcan, H. FerdiGerçel; Preparation of activated carbon from a renewable bio-plant of Euphorbia rigida by H2SO4 activation and its adsorption behavior in aqueous solutions, Applied Surface Science253 (2007) 4843-4852.

[16]Ali H. Jawad, R.Razuan, Jimmy Nelson Appaturi, Lee D. Wilson; Adsorption and mechanism study for methylene blue dye removal with carbonized watermelon (Citrulluslanatus) rind prepared via one-step liquid phase H2SO4 activation, Surfaces and Interfaces16 (2019) 76-84.

[17]Alexander M.Puziy, Olga I. Poddubnaya, Amelia Martínez-Alonso, Alberto Castro-Muñiz, Fabian Suárez-García, Juan M.D.Tascón; Oxygen and phosphorus enriched carbons from lignocellulosic material, Carbon45 (2007) 1941-1950.

[18]Nan Zhou, Yifan Wang, Liyang Huang, Jingang Yu, Huanli Chen, Jiajie Tang, FengjuanXu, Xiangyang Lu, Mei-e Zhong, ZhiZhou; In situ modification provided by a novel wet pyrolysis system to enhance surface properties of biochar for lead immobilization, Colloids and Surfaces A: Physicochemical and Engineering Aspects570 (2019) 39-47.

[19] S. Kushwaha, H. Soni, B. Sreedhar, P. Padmaja; Efficient valorisation of palm shell powder to bio-sorbents for copper remediation from aqueous solutions, Journal of Environmental Chemical Engineering 5 (2017) 2480-2487.

[20]N. A. H. MohamadZaidi, L. B. L. Lim, A. Usman; Enhancing *adsorption* of Pb(II) from aqueous solution by *NaOH* and EDTA *modified*Artocarpusodoratissimus leaves, Journal of Environmental Chemical Engineering, 6 (2018) 7172-7184

[21]Xu P., Zeng G., Huang D., Hu S., Feng C., Lai C., Zhao M., Huang C., Li N., Wei Z, Xie G.; Synthesis of iron oxide nanoparticles and their application in *Phanerochaetechrysosporium* immobilization for Pb(II) removal, Colloids Surf A PhysicochemEng Aspects, 419 (2013), pp. 147-155.

[22]Priya Saharan, Ashok K. Sharma, Vinit Kumar, InduKaushal; Multifunctional CNT supported metal doped $MnO_2$ composite for adsorptive removal of anionic dye and thiourea sensing, Materials Chemistry and Physics 221 (2019) 239–249.

[23] T. Hajeeth, K. Vijayalakshmi, T. Gomathi, P.N. Sudha; Removal of Cu(II) and Ni(II) using

cellulose extracted from sisal fiber and cellulose-g-acrylic acid copolymer, Int J BiolMacromol, 62 (2013), pp. 59-65

[24] Deepak Tiwari, HaripadaBhunia, Pramod K. Bajpai; Adsorptionof $CO_2$onKOHactivated, N-enrichedcarbonderivedfromureaformaldehydere sin*:* kinetics, isotherm and thermodynamicstudies, Applied Surface Science, Volume 439, 1 May 2018, Pages 760-771.

[25]DivyamJhaa, N.M. Mubarakb, Mohd. BelalHaidera, Rakesh Kumara, M.S. Balathanigaimania, J.N. Sahu; Adsorptive removal of dibenzothiophene from diesel fuel using microwave synthesized carbon nanomaterials, Fuel 244 (2019) 132–139.

[26]Li Wang, Jingyi Wang, Chi He, Wei Lyu, Wenlong Zhang, Wei Yan, Liu Yang; Development of rare earth element doped magnetic biochars with enhanced phosphate adsorption performance, Colloids and Surfaces A 561 (2019) 236–243.

[27]ElhamBoorboorAzimi, AlirezaBadiei, Jahan B. Ghasemi; Efficient removal of malachite green from wastewater by using boron-doped mesoporous carbon nitride, Applied Surface Science 469 (2019) 236–245.

[28]AyyubKhawar, ZaheerAslam, Abdul Zahir, Imran Akbar, Aamir Abbas; Synthesis of Femur extracted hydroxyapatite reinforced nanocomposite and its application for Pb(II) ions abatement from aqueous phase, International Journal of Biological Macromolecules 122 (2019) 667–676.

[29]Aola Supong, Parimal Chandra Bhomick, Mridushmita Baruah, Chubaakum Pongener, DipakSinha; Adsorptive removal of Bisphenol A by biomass activated carbon and insights into the adsorption mechanism through density functional theory calculations, Sustainable Chemistry and Pharmacy, Volume 13, September 2019, Article 100159.

[30]Soh-Fong Lim & Agnes Yung Weng Lee; Environ Sci Pollut Res (2015) 22:10144–10158.

[31]Drishti Bhatia, Dipaloy Datta, Abhishek Joshi, Sagar Gupta, Yogesh Gote; Adsorption of isonicotinic acid from aqueous solution using multi-walled carbon nanotubes/Fe3O4, Journal of Molecular Liquids 276 (2019) 163–169 Journal of Molecular Liquids 276 (2019) 163–169.

[32]Yuhao Zhou, Zhe Liu, Arixin Bo, Tana Tana, Huaiyong Zhu; Simultaneous removal of cationic and anionic heavy metal contaminants from electroplating effluent by hydrotalcite adsorbent with disulfide (S2−) intercalation, Journal of Hazardous Materials, Volume 382, 15 January 2020, Article 121111

[33] G. Zhou, J. Luo, C. Liu, L. Chu, J. Crittenden; Efficient heavy metal removal from industrial melting effluent using fixed-bed process based on porous hydrogel adsorbents, Water Res., 131 (2018) (2018), pp. 246-254.

[34] H. Sharififard, Z.H. Shahraki, E. Rezvanpanah, S.H. Rad; A novel natural chitosan/activated carbon/iron bio-nanocomposite: Sonochemical synthesis, characterization, and application for cadmium removal in batch and continuous adsorption process, Bioresour. Technol., 270 (2018), pp. 562-569.

[35] B. Das, N.K. Mondal, R. Bhaumik, P. Roy; Insight into adsorption equilibrium, kinetics and thermodynamics of lead onto alluvial soil, Int. J. Environ. Sci. Technol. (Tehran), 11 (2014), pp. 1101-1114.

[36]Yasser Hannachi, AfifaHafidh, SalwaAyed; Effectiveness of novel xerogelsadsorbents for cadmium uptake from aqueoussolution in batch and column modes: Synthesis, characterization, equilibrium, and mechanismanalysis, Chemical Engineering Research and Design, Volume 143, March 2019, Pages 11-23

[37] Rainwater, F.H. and L.L. Thatcher, 1960. Methods for collection and analysis of water samples.U.S. Geol. Surv.Water Supply. Paper No.1454, U.S.A., p: 301.

[38]Fishman, M.J. and L.C. Friedman, 1985. Methods for determination of inorganic substances in water and fluvial sediments.U.S. Geol. Surv. Book 5, Chapter A1. Open File Report, 85-495, Denver, Colorado, U.S.A.

[39]J. Zhang, S. Chen, H. Zhang, X. Wang; Removal behaviors and mechanisms of hexavalent chromium from aqueous solution by cephalosporin residue and derived chars, Bioresource and Technology., 238 (2017) 484.

[40] Abhay Prakash Rawat, D. P. Singh; Application of biosorbents derived from agro-waste in removal of dyes and heavy metals from aqueous solutions, Ecotoxicology and Environmental Safety 176 (2019) 27-33.

[41] E. Fosso-Kankeu, H. Mittal, F. Waanders, S.S. Ray Thermodynamic properties and adsorption behavior of hydrogel nanocomposites for cadmium removal from mine effluents, J. Ind. Eng. Chem., 48 (2017) 151-161,

[42]Amal Djelad, Adel Mokhtar, Amine Khelifa, Abdelkader Bengueddach, Mohamed Sassi; Alginate-whey an effective and green adsorbent for crystal violet removal: Kinetic, thermodynamic and mechanism studies, International Journal of Biological Macromolecules 139 (2019) 944-954.

[43]G. Zhou, J. Luo, C. Liu, L. Chu, J. Crittenden; Efficient heavy metal removal from industrial melting effluent using fixed-bed process based on porous hydrogel adsorbents, Water Research., 131 (2018) (2018) 246-254,

**الملخص العربى**

# تحضير الكربون المنشط من راتنجات التبادل الأيوني وتطبيقه لإزالة المنجنيز من المياه الجوفية

**عبد السميع سويلم[1] ، يحيي جدامي[2] ، احمد الشاهد[2]**

**1- قسم الكيمياء ، كلية العلوم ، جامعة الازهر ، القاهرة ، مصر**

**2- قسم الهيدروجيوكيمياء ، مركز بحوث الصحراء ، المطرية ، القاهرة ، مصر**

تهدف هذه الدراسة الى تحضير مادة ماصة من الكربون المنشط (S-AC,P-AC,OH-AC) وذلك من نفايات البوليسترين ديفينيل بنزين تحت درجات حرارة مختلفة (450 ، 900 درجة مئوية) ومواد تنشيط ($H_2SO_4$,$H_3PO_4$,NaOH). تم اجراء التجارب للوقوف على خواص المادة المحضرة ثم تم استخدام هذة المواد كمواد ماصة لإزالة المنغنيز من المياه الجوفية الملوثة. وتشير نتائج FTIR إلى أن عملية الارتباط بين المادة الماصة والمنجنيز تتم على سطح المادة الماصة. وهناك عدة عوامل مختلفة تؤثر على عملية الامتصاص تم اختبارها مثل الرقم الهيدروجيني، جرعة الممتزات ، وقت الاتصال ، ودرجة الحرارة والتركيز الأولي.وأظهرت النتائج أن قدرة امتصاص المنغنيز تتناقص مع زيادة درجة حرارة الكربنة (900 درجة مئوية) ومواد التفعيل تترتب من حيث التأثيرالى $H_2SO_4$> $H_3PO_4$>NaOH. حركيًا ، تبين أن درجة حرارة التنشيط التي تبلغ 450 درجة مئوية هي أفضل درجة حرارة لتفعيل الكربون الممتص. يعتبر The pseudo-first-order modelمناسبًا للتنبؤ بعملية الامتزاز للمنجنيز على P-AC 900ºC,OH-AC 900ºC في حين نجد أن الموديل الأخر P-AC 450ºC,The pseudo-second-order modelيكون مناسب للتنبؤ بعملية الامتزاز للمنجنيز على كل من S-AC 450ºC,S-AC 900ºC,OH-AC 450ºC,OH-AC 900ºC. أكدت الحسابات الديناميكية الحرارية أن امتصاص المنجنيز على كل منS-AC,P-AC كان عملية ماصة للحرارة بينما على OH-AC كانت عملية طاردة للحرارة. تشير قيم $\Delta G^o$ السالبة إلى امتزاز المنغنيز يكون إيجابي وعفوي على S-AC في درجات الحرارة الثلاث306, 316, 320K في حين أن امتزاز المنغنيز بواسطة كل من P-AC,OH-AC في جميع درجات الحرارة الأربع كان غير عفوي. أخيرًا ، يمكن اعتبار S-AC,P-AC,OH-AC المحضر بمثابة مادة ماصة فعالة لإزالة المنجنيز من المياه الجوفية الملوثة. بينما تشير النتائج إلى أن S-AC يتمتع بقدرات امتصاص عالية للمنجنيز مقارنة مع المواد ماصة ألأخرى مثل P-AC,OH-AC. لذلك يمكن استخدام S-AC 450ºC في وحدات معالجة المياه الجوفية الملوثه.